Beam quality of a non-ideal atom laser

J.-F. Riou, W. Guerin, Y. Le Coq, M. Fauquembergue, Philippe Bouyer, Vincent Josse, Alain Aspect

Beam quality of a non-ideal atom laser

J.-F. Riou,* W. Guerin, Y. Le Coq†, M. Fauquembergue, V. Josse, P. Bouyer, and A. Aspect
Groupe d'Optique Atomique, Laboratoire Charles Fabry de l'Institut d'Optique,
UMRA 8501 du CNRS,
Bât. 503, Campus universitaire d'Orsay,
91403 ORSAY CEDEX, FRANCE
(Dated: September 14, 2005)

We have measured the effect of interactions on atom-laser beam quality. We observe a transverse structure containing caustics that vary with the density within the residing Bose-Einstein Condensate. Using WKB approximation, Fresnel-Kirchhoff integral formalism and atom-optical ABCD matrices, we are able to predict analytically these profiles. This allows us to characterize the quality of the non-ideal atom-laser beam by a generalized M^2 factor defined in analogy to photon lasers.

PACS numbers: 03.75.Pp, 39.20.+q, 42.60.Jf,41.85.Ew

Optical lasers have had an enormous impact on science and technology, due to their high brightness and coherence. The high spatial quality of the beam and the little spread when propagating in the far-field allow applications ranging from the focusing onto tiny spots and optical lithography [1] to collimation over astronomic distances [2]. In atomic physics, Bose-Einstein condensates (BEC) of trapped atoms [3] are an atomic equivalent to photons stored in a single mode of an optical cavity, from which a coherent matter wave (atom laser) can be extracted [4, 5]. The possibility of creating continuous atom laser [6] promises spectacular improvements in future applications, as for instance in the atom-interferometer-based inertial sensors [7], atom-chip based interferometers [8, 9] or in precision atomic lithography [10]. These improvements will benefit from the high brightness, strong collimation [11] and focusing ability of such beam [12, 13]. Nevertheless these properties depend drastically on the quality of the transverse profile whose characterization, as for the optical lasers [14], is of crucial importance.

In atom optics, interactions give rise to non-linear effects orders of magnitude larger than in standard photon optics. They are at the origin of numerous phenomena that can be advantageous in certain circumstances, as, for example, soliton propagation [15] or atomic four-wave mixing [16]. However, it is also a source of degradation of beam quality, analogous to thermal or non-linear effects that can cause significant *decollimation* as well as optical aberrations in optical lasers [17]. Indeed, it has already been shown that the trapped BEC weakly interacting with the outcoupled atom-laser beam can act as an effective thin-lens which leads to the divergence of the atom laser [18]. When this interaction increases, more dramatic degradations of the beam are predicted [19] with the apparition of a transverse modulation of the atom-laser beam intensity.

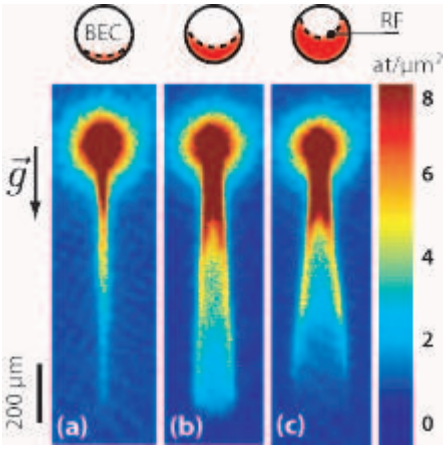

FIG. 1: Absorption images of a non-ideal atom laser, corresponding to density integration along the elongated axis x of the BEC. The figures correspond to different height of RF-outcoupler detunings with respect to the bottom of the BEC: (a) -0.37 μm (b) $-2,22$ μm (c) -3.55 μm. The graph above shows the RF-outcoupler (dashed line) and the BEC slice (red) which is crossed by the atom laser and results in the observation of caustics. The field of view is $350\,\mu\text{m} \times 1200\,\mu\text{m}$ for each image.

In order to quantitatively qualify the *atom-laser beam quality*, it is tempting to take advantage of the methods developed in optics to deal with non-ideal laser beams. Following the initial work of Siegman [20] who introduced the quality factor M^2 which is proportional to the space-beam-width (divergence $\times$ size) product at the waist, it is natural to extend its definition to atom optics as

$$\Delta x\ \Delta k_x\ =\ \frac{M^2}{2}, \tag{1}$$

where Δx characterizes the size and $\Delta k_x = \Delta p_x/\hbar$, with Δp_x the width of the momentum distribution along x. Equation (1) plays the same role as the Heisenberg dis-

†Present address: NIST, Mailcode 847.00, 325 Broadway, Boulder, CO 80305-3328 (U.S.A.)

persion relation: it expresses how many times the beam deviates from a minimal state.

In this letter, we experimentally and theoretically study the quality factor M^2 of a non-ideal atom-laser beam. First, we present our experimental investigation of the structures that appear in the transverse profile (see Fig. 1) [21]. We show that they are indeed influenced by the interactions between the trapped BEC and the outcoupled beam. Then, using an approach, based on the WKB approximation and the Fresnel-Kirchhoff integral formalism, we are able to calculate analytical profiles which agree with our experimental observations. This allows us to generalize concepts introduced in [20] for photon laser and to calculate the quality factor M^2 which can then be used in combination with the paraxial ABCD matrices for gaussian beams [22] to describe the propagation of the non-ideal beam. Finally, we present a study of the M^2 quality factor as a function of the thickness of the interaction-induced lens.

Our experiment relates to atom lasers obtained by radio frequency (RF) outcoupling from a BEC [5, 23]. The experimental setup for producing Bose-Einstein condensates of ^{87}Rb is described in detail in [25]. Briefly, a Zeeman-slowed atomic beam loads a magneto-optical trap in a glass cell. About 2×10^8 atoms are transferred in the $|F, m_F\rangle = |1, -1\rangle$ state to a Ioffe-Pritchard magnetic trap , which is subsequently compressed to oscillation frequencies of $\omega_x = 2\pi \times 8$ Hz and $\omega_{y,z} = 2\pi \times 330$ Hz in the dipole and quadrupole directions respectively. A 25 s RF-induced evaporative cooling ramp results in a pure condensate of $N = 10^6$ atoms, cigar-shaped along the x axis.

The atom laser is extracted from the BEC by applying a RF field a few kHz from the bottom of the trap, in order to couple the trapped state to the weakly antitrapped state $|1, 0\rangle$. The subsequent atomic beam falls under the effect of both gravity $-mgz$ and second order Zeeman effect $V = -m\omega^2(y^2 + (z + \varrho)^2)/2$ [24] with $\omega = 2\pi \times 20$ Hz and $z = -\varrho$ corresponds to the center of the magnetic trap (see Fig. 2a). The RF-outcoupler amplitude is weak enough to avoid perturbation of the condensate so that the laser dynamics is quasi-stationary [23]. Since the BEC is displaced vertically by the gravitational sag, the value of the RF-outcoupler frequency $\nu_{\rm RF}$ defines the height where the laser is extracted [5]. After 10 ms of operation, the fields are switched off and absorption imaging is taken after 1 ms of free fall with a measured spatial resolution of 6 μm. The line of sight is along the weak x axis so that we observe the transverse profile of the atom laser in the $\{y, z\}$ plane.

Typical images are shown in figure 1. A transverse structure, similar to the predictions in [19], is clearly visible in figures 1b and 1c. The laser beam quality degrades as the RF-outcoupler is higher in the BEC (i.e. the laser beam crosses more condensate), supporting the interpretation that this effect is due to the strong repulsive interaction between the BEC and the laser. Indeed, this effect can be understood with a semi-classical picture. The mean-field interaction results in an inverted harmonic potential of frequencies ω_i (in the directions $i = x, y, z$) which are fixed by the magnetic confinement [18, 27]. The interaction potential expels the atoms transversally, as illustrated in Fig. 2. Because of the finite size of the condensate, the trajectories initially at the center of the beam experience more mean-field repulsion than the trajectories initially at the border. This results in accumulation at the edge of the laser [19], in a similar manner to caustics in optics. This picture enables a clear physical understanding of the behaviour observed in figure 1: if $\nu_{\rm RF}$ is chosen so that extraction is located at the bottom of the BEC (Fig. 1a), the effect of interaction is negligible and one gets a collimated beam. As the RF outcoupler moves upwards (Fig. 1b and 1c), a thicker part of the condensate acts on the laser and *defocusing*, then *caustics*, appear. We verified that when decreasing the transverse confinement, the atom laser is collimated at any RF value [28].

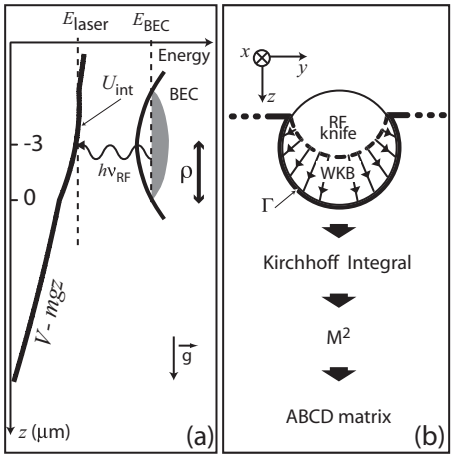

FIG. 2: (a) Principle of the RF-outcoupler : the radio-frequency $\nu_{RF} = (E_{\rm BEC} - E_{\rm laser})/h$ selects the initial position of the extracted atom-laser beam. The laser is then subjected to the condensate mean-field potential $U_{\rm int}$, to the quadratic Zeeman effect V and to gravity $-mgz$. For the sake of clarity, V has been exaggerated on the graph. (b) Representation of the two-dimensional theoretical treatment: inside the condensate, phase accumulation along atomic rays determines the laser wavefront at the BEC output. From there, a Fresnel-Kirchhoff integral on the contour Γ is used to calculate the stationary laser wavefunction at any point below the condensate. As soon as the beam enters the paraxial regime we calculate the M^2 quality factor and use ABCD matrix formalism.

The above discussion is not sufficient to describe quantitatively the details of the profiles of the non-ideal atom laser. However, methods developed initially in the context of photon optics can be extended to atom optics. These methods enable a full calculation of the atom-laser propagation together with its characterization by means

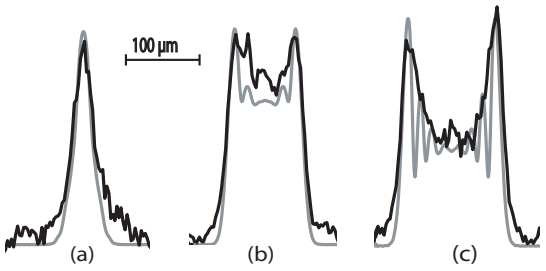

FIG. 3: Comparison of experimental (black) and theoretical (gray) column densities after 600 microns of propagation for the same RF-outcoupler height as in Fig. 1. Theoretical figures take into account the integration along the line of sight and the resolution of the imaging system.

of the quality factor M^2. In general, one cannot restrict the analysis to paraxial propagation [18] unless the transverse kinetic energy is smaller than the longitudinal one, which, in particular, is not verified in the vicinity of the BEC. We thus split the evolution into three steps that require different formalisms: WKB in the BEC, Fresnel-Kirchhoff integral at the output of the condensate and, where paraxial approximation is valid, ABCD matrices. In all the following, we also neglect mean-field interactions within the atom-laser beam since it is very dilute compared to the initial BEC source. In addition, the condensate is elongated along the x axis, so that the forces along this direction are negligible and we consider only the dynamics in the y, z plane.

First, we consider that the atoms extracted from the condensate by the RF-outcoupler start at zero speed from $\mathbf{r}_0$ along the equipotential and thus trajectories are straight lines (see Fig. 2b). At this stage, we neglect diffraction since the travelling time τ_0 needed to exit is small: the beam profile $\psi(\mathbf{r}_1)$ at the BEC border is obtained by accumulating the phase along the classical path

$$\psi(\mathbf{r}_1) \propto \frac{1}{\sinh(\omega_z \tau_0)} e^{i\int_{\mathbf{r}_0}^{\mathbf{r}_1} \mathbf{k}(\mathbf{r})\cdot d\mathbf{r}} \psi_{\mathrm{BEC}}(\mathbf{r}_0), \qquad (2)$$

where ψ_{BEC} is the condensate wavefunction. The prefactor in Eq. (2) ensures the conservation of the flux.

Second, because the atom laser can be considered to be in a stationary state, we propagate the wavefunction for a given energy E which satisfies the time-independent Schrödinger equation in the potential $V - mgz$. Since this equation is analogous to the Helmoltz equation [29, 30] in optics, Fresnel-Kirchhoff integral formalism can be generalized to atom optics as [31]

$$\psi(\mathbf{r}) \propto \oint_\Gamma d\mathbf{l}_1 \cdot \left[G_E \nabla_1 \psi(\mathbf{r}_1) - \psi(\mathbf{r}_1) \nabla_1 G_E \right]. \qquad (3)$$

We choose the contour Γ along the condensate border and close it at infinity (see Fig. 2). The time-independent Green's function $G_E(\mathbf{r}, \mathbf{r}_1)$ is analytically evaluated from the time-domain Fourier transform of the Feynman propagator $K(\mathbf{r}, \mathbf{r}_1, \tau)$ [31, 32] calculated by means of the Van Vleck formula [33]. Using $\psi(\mathbf{r_1})$ from equation (2), the wavefunction $\psi(\mathbf{r})$ is then known at any location $\mathbf{r}$. We verified the excellent agreement of this model with a full numerical integration of the Gross-Pitaevskii equation. We show a comparison of our experimental observations with this theory in Fig. 3. The theoretical profiles correspond to 600 μm of propagation and take into account the optical measurement process. The only adjustable parameter is the amplitude of the profile. The predicted fringes, which physically result from the interference of different quantum paths [19], are not observed. This could be attributed, for example, to small oscillations of the initial BEC [13] that may wash out the fringe contrast.

As previously stressed, this method is demanded only for the early stages of the propagation. As soon as the paraxial approximation becomes valid, the ABCD matrix formalism can be used to efficiently describe the propagation the beam. In order to study the change in the width of the beam in this regime, we define, following [20], a generalized complex radius of curvature

$$\frac{1}{q(\xi)} = \mathcal{C}(\xi) + \frac{i\mathrm{M}^2}{2\sigma_y^2(\xi)}, \qquad (4)$$

where σ_y is the rms width of the density profile, $\xi(t)$ a reduced spatial variable which describes the time evolution of the beam so that $\xi = 0$ corresponds to the position of the waist. Equation (4) involves an invariant coefficient, the beam-quality factor M^2 [20], as defined in Eq. (1). This coefficient, as well as the effective curvature $\mathcal{C}(\xi)$, can be extracted from the wavefront in the paraxial domain, as explained in [34]. In optics, this generalized complex radius obeys the same ABCD propagation rules as does a Gaussian beam of the same real beam size, if the wavelength λ is changed to $M^2\lambda$ [22]. Similarly, the complex radius $q(\xi)$ follows here the ABCD law for matter-waves [18], and we obtain the rms width

$$\sigma_y^2(\xi) = \sigma_{y0}^2 \cosh^2(\xi) + \left(\frac{\mathrm{M}^2\hbar}{2m\omega}\right)^2 \frac{\sinh^2(\xi)}{\sigma_{y0}^2}, \qquad (5)$$

where σ_{y0} is taken at the waist.

This generalized Rayleigh formula allows to measure M^2. In figure 4, the evolution of the transverse rms width versus propagation ξ, taken from experimental images, is compared to the one calculated with Eq. (5), where σ_{y0} is given by our model. For a chosen RF-outcoupler position, we fit the variation of the width with a single free parameter M^2 as illustrated in the inset. Again, good agreement between theory and experiment is found as we quantify the degradation of atom laser profile for each RF value.

In conclusion, we have characterized the transverse profile of an atom laser. We demonstrated that, in our case, interactions when crossing the condensate are a critical contributor to the observed degradation of the

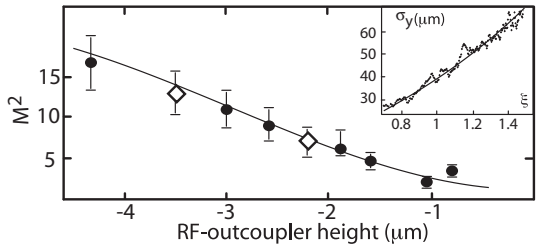

FIG. 4: M^2 quality factor vs RF-outcoupler distance from the bottom of the BEC: theory (solid line), experimental points (circles). The two diamonds represent the M^2 for the two non-ideal atom lasers shown in figure 1b and 1c. The RF-outcoupler position (i.e. the RF detuning from the bottom of the BEC) is calibrated by the number of outcoupled atoms. Inset: typical fit of the laser rms size with the generalized Rayleigh formula (Eq. 5) for RF-outcoupler position -3.55 μm.

beam. We showed that the beam-quality factor M^2, initially introduced by Siegman [20] for photon laser, is as well a fruitful concept for characterizing the propagation of an atom laser. For instance, it determines the minimal focusing size that can be achieved with atomic lenses [13]. The analogy between atom-laser and photon-lasers beams, both fully coherent, propagating waves, is emphasized by the success of a model obtained by generalization of the standard treatment of optical laser beams. This model allows to predict the factor M^2 of an atom laser. This is of essential importance in view of future applications of coherent matter-waves as, for example, when strong focusing will be needed for coupling atom lasers onto to guiding structures of atomic chips [35].

The authors would like to thank S. Rangwala for his help in the early stage of the experiment, L. Sanchez-Palencia and I. Bouchoule for fruitful discussions and R. Nyman for careful reading of the manuscript. This experiment could not have been done without the help of A. Villing and F. Moron. This work is supported by CNES (DA:10030054), CNRS, DGA (contract 9934050 and 0434042), LNE, EU (grants IST-2001-38863, MRTN-CT-2003-505032 and FINAQS STREP), INTAS (contract 211-855) and QUDEDIS.

* Electronic address: Jean-Felix.Riou@iota.u-psud.fr; URL: `http://atomoptic.iota.u-psud.fr`

[1] R. Ito and S. Okazaki, Nature. **406**, 1027 (2000).
[2] P. L. Bender *et al.*, Science **182**, 229 (1973).
[3] M.H. Anderson *et al.*, Science **269**, 198 (1995); K.B. Davis *et al*, Phys. Rev. Lett. **75**, 3969 (1995); C.C. Bradley *et al*, Phys. Rev. Lett. **75**, 1687 (1995).
[4] M.-O. Mewes *et al.*, Phys. Rev. Lett. **78**, 582 (1997); B.P. Anderson and M. A. Kasevich *et al.* , Science **282**, 1686 (1998); E.W. Hagley *et al*, Science **283**, 1706 (1999).
[5] I. Bloch, T. W. Hänsch and T. Esslinger, Phys. Rev. Lett. **82**, 3008 (1999).
[6] A. P. Chikkatur *et al.*, Science, **296**, 2193, 2002; T. Lahaye *et al.*, arXiv: cond-mat/0505709 (2005).
[7] P. Bouyer and M.A. Kasevich, Phys. Rev. A **56**, R1083 (1997).
[8] Y.-J. Wang *et al.*, Phys. Rev. Lett. **94**, 090405 (2005).
[9] Y. Shin *et al.*, Phys. Rev. A **72**, 021604(R) (2005).
[10] E. te Sligte *et al.*, Appl. Phys. Lett., **85** (19), 4493 (2004); G. Myszkiewicz *et al.*, Appl. Phys. Lett., **85** (17), 3842 (2004).
[11] Y. Le Coq *et al.*, arXiv: cond-mat/0501520 (2005).
[12] I. Bloch *et al.*, Phys. Rev. Lett., **87** 030401, (2001).
[13] I. Schvarchuck *et al.*, Phys. Rev. Lett., **89**, 270404, (2002); A S Arnold, C MacCormick and M G Boshier, J. Phys. B: At. Mol. Opt. Phys. **37** 485, (2004).
[14] A.E. Siegman, in *Solid State Lasers : New Developments and Applications*, edited by M. Inguscio and R. Wallenstein, (Plenum Press, New York, 1993) p.13.
[15] S. Burger *et al.*, Phys. Rev. Lett., **83**, 5198 (1999); Denschlag *et al*, Science, **287**, 97 (2000); L. Khaykovich *et al*, Science, **296**, 1290-1293 (2002).
[16] L. Deng *et al.*, Nature, **398**, 218 (1999); J.M. Vogels, K. Xu, and W. Ketterle Phys. Rev. Lett. **89**, 020401 (2002).
[17] S. A. Akhmanov, R. V. Khokhlov and A. P. Sukhorukov, *Laser Handbook*, North-Holland Amsterdam (1972).
[18] Y. Le Coq *et al.*, Phys. Rev. Lett. **87**, 170403 (2001).
[19] T. Busch *et al.*, Phys. Rev. A **65**, 043615 (2002).
[20] A. E. Siegman, IEEE J. Quantum Electron. **27**, 1146 (1991).
[21] While writing this paper, we have been informed that similar observations had been reported by the group of T. Esslinger in M. Köhl *et al.*, arXiv:cond-mat/0508778v1 (2005).
[22] P.A. Belanger, Optics Lett. **16**, 196 (1991).
[23] F.Gerbier, P. Bouyer and A. Aspect, Phys. Rev. Lett. **86**, 4729 (2001); Phys. Rev. Lett. **93**, 059905(E) (2004).
[24] B. Desruelle *et al.*, Phys. Rev. A **60**, R1759 (1999).
[25] M. Fauquembergue *et al.*, arXiv:cond-mat/0507129v2 (2005).
[26] I. Bloch, T. W. Hänsch and T. Esslinger, Nature **403**, 166 (2000).
[27] F. Dalfovo *et al.*, Rev. Mod. Phys. **71**, 463 (1999).
[28] We also verified that this effect is far from sensitive to the condensate atom number, since, in the Thomas-Fermi regime, the size of the condensate, and thus the part acting on the atom laser varies as $N^{1/5}$ [27].
[29] M. Born and E. Wolf, *Principles of optics*, Cambridge Univ. Press (7th edition) (2002).
[30] C. Henkel, J.-Y. Courtois and A. Aspect, J. Phys. II France **4**, 1955 (1994); C. Henkel, http://tel.ccsd.cnrs.fr, tel-00006757 (1996).
[31] Ch. J. Bordé in *Fundamental Systems in Quantum Optics*, edited by J. Dalibard (Elsevier 1991); Ch. J. Bordé C.R. Acad. Sci. Paris, t.2;série IV 509-530 (2001).
[32] R. P. Feynman and A. R. Hibbs, *Quantum mechanics and path integrals*, McGraw-Hill (1965).
[33] J. H. Van Vleck , Proc. Natl. Acad. Sci. USA 14 178-188 (1928).
[34] A.E. Siegman, *Lasers*, Un. Sci. Books, Mill Valley, California (1986).
[35] *Special Issue - Atom chips: manipulating atoms and molecules with microfabricated structures*, The European Physical Journal D **35** No. 1 (2005).